Supplementary information

Fast divalent conduction in $M(BH_4)_2$–$12H_2O$ (M = Zn, Mg) complex hydrides: effects of rapid crystal water exchange and application for solid-state electrolyte

Kazuaki Kisu,[a] Arunkumar Dorai,[a,b] Sangryun Kim,[c] Riku Hamada,[a] Akichika Kumatani,[d,e,f,g] Yoshiko Horiguchi,[d] Ryuhei Sato,[d] Kartik Sau,[d] Shigeyuki Takagi,[a] and Shin-ichi Orimo [a,d*]*

a. *Institute for Materials Research (IMR), Tohoku University, Katahira 2-1-1, Aoba-ku, Sendai 980-8577, Japan, E-mail: kazuaki.kisu.b2@tohoku.ac.jp*
b. *Institute of Multidisciplinary Research for Advanced Materials, Tohoku University, 2-1-1 Katahira, Aoba-ku, Sendai, 980-8577, Japan.*
c. *Graduate School of Energy Convergence, Gwangju Institute of Science and Technology (GIST), 123 Cheomdangwagi-ro, Buk-gu, Gwangju 61005, Republic of Korea*
d. *Advanced Institute for Materials Research (WPI-AIMR), Tohoku University, Katahira 2-1-1, Aoba-ku, Sendai 980-8577, Japan*
e. *WPI-International Center for Materials Nanoarchitectonics (WPI-MANA), National Institute for Materials Science (NIMS), Tsukuba, Ibaraki 305-0044, Japan.*
f. *Graduate School of Environmental Studies, Tohoku University, Sendai 980-856, Japan.*
g. *Center for Science and Innovation in Spintronics (CSIS), Tohoku University, Sendai 980-8577, Japan.*

E-mail: kazuaki.kisu.b2@tohoku.ac.jp; shin-ichi.orimo.a6@tohoku.ac.jp

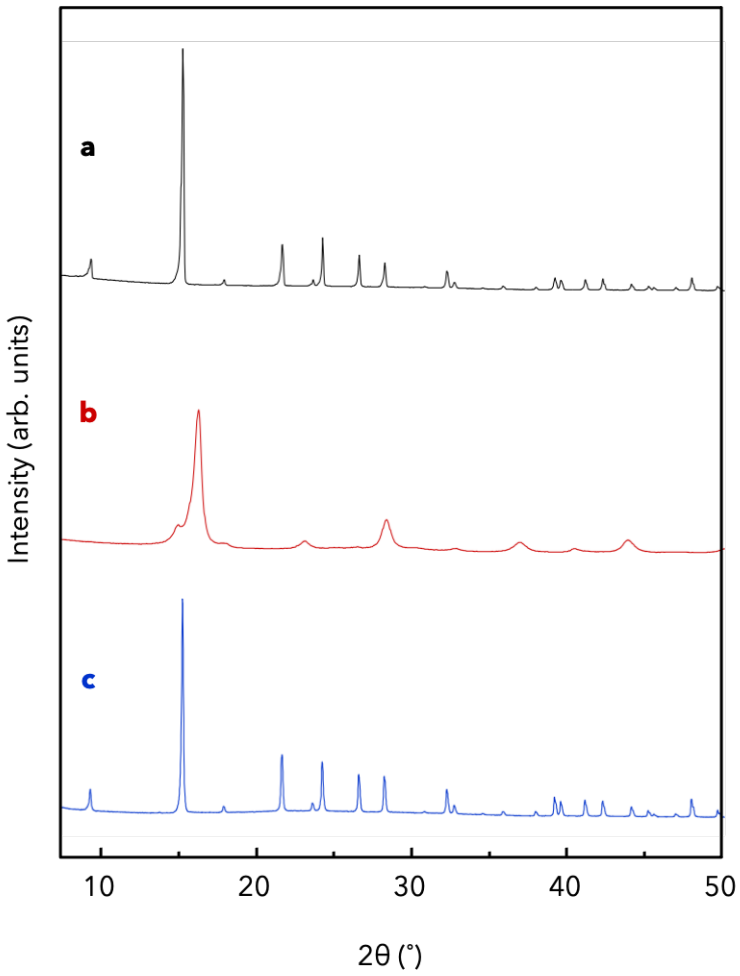

Figure S1. (a) XRD patterns for $ZnB_{12}H_{12}$-$12H_2O$, (b) $ZnB_{12}H_{12}$ anhydrous, (c) rehydrated $ZnB_{12}H_{12}$ anhydrous.

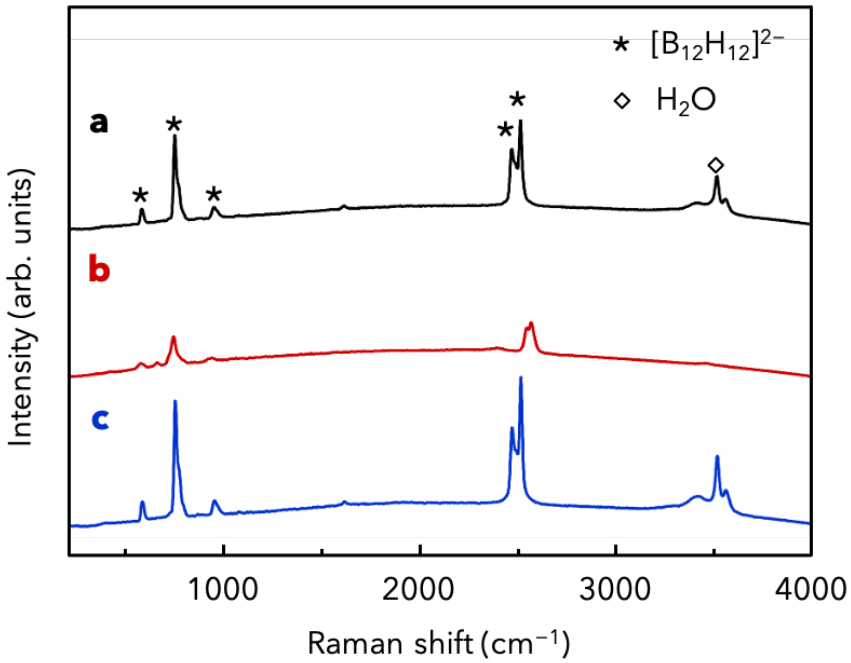

Figure S2. (a) Raman spectra for $ZnB_{12}H_{12}$–$12H_2O$, (b) $ZnB_{12}H_{12}$ anhydrous, (c) rehydrated anhydrous $ZnB_{12}H_{12}$.

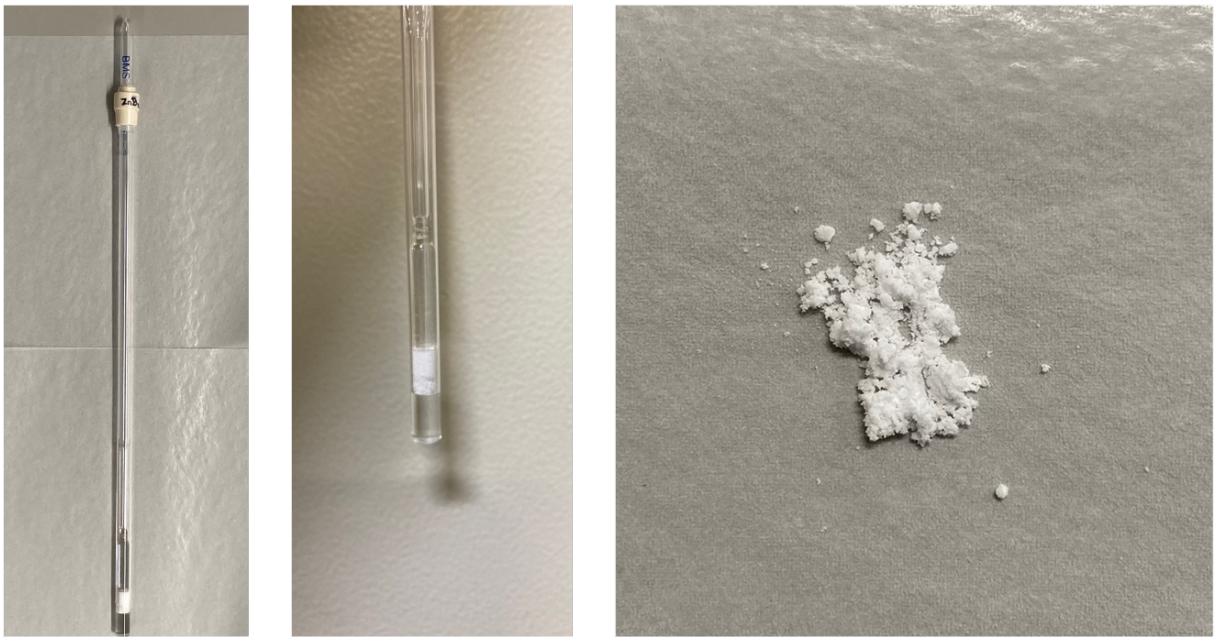

Figure S3. $ZnB_{12}H_{12}$–$12H_2O$ sample photos without melting after ^{67}Zn NMR measurements.

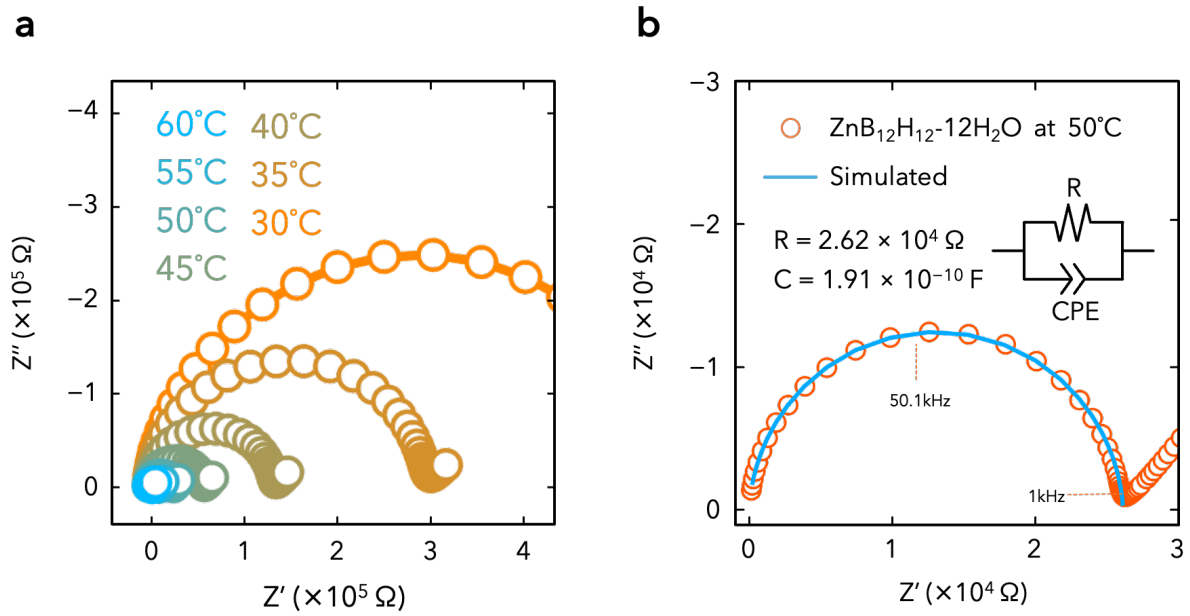

Figure S4. (a) Nyquist plots recorded for $ZnB_{12}H_{12}$–$12H_2O$ between 30 and 60 °C. (b) Nyquist plot and simulated curve for $ZnB_{12}H_{12}$–$12H_2O$. The inset shows the equivalent circuit used for fitting.

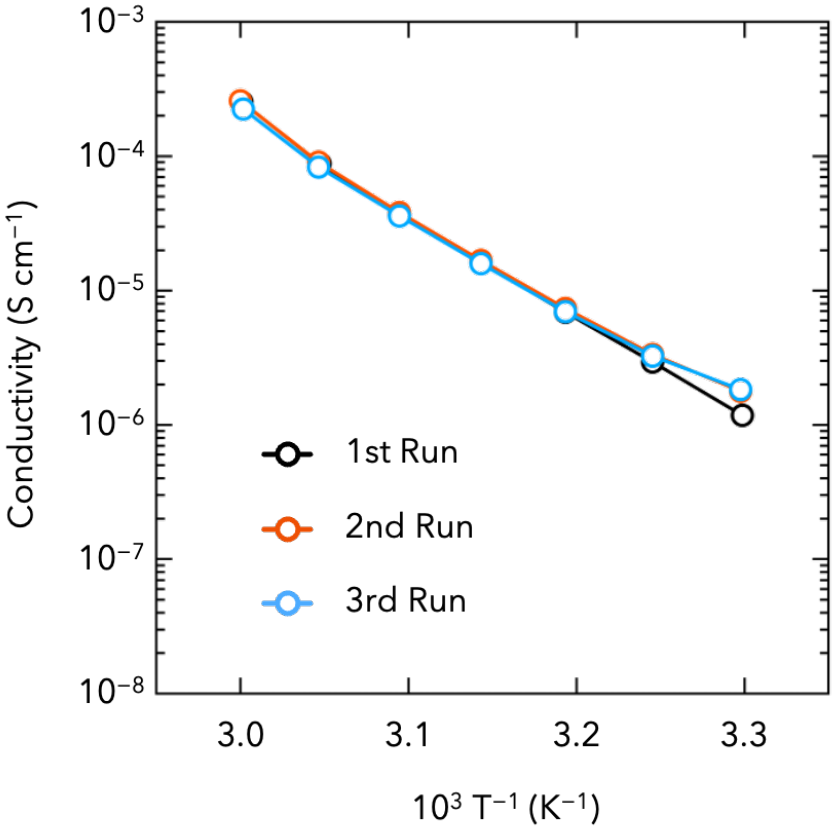

Figure S5. Ionic conductivity of $ZnB_{12}H_{12}$–$12H_2O$ obtained by impedance spectroscopy. Black, orange, and blue circles represent the results of the first, second, and third runs, respectively.

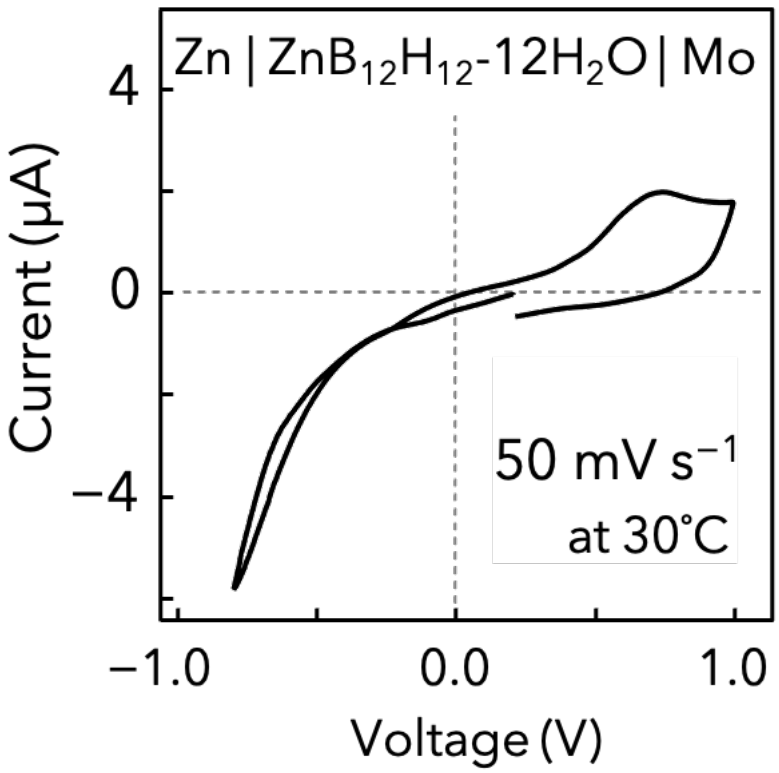

Figure S6. Cyclic voltammogram of Zn | $ZnB_{12}H_{12}$–$12H_2O$ | Mo recorded at a temperature of 30 °C and a scan rate of 50 mV s^{-1} within a voltage range of −0.8 to 1.0 V (*vs.* Zn^{2+}/Zn).

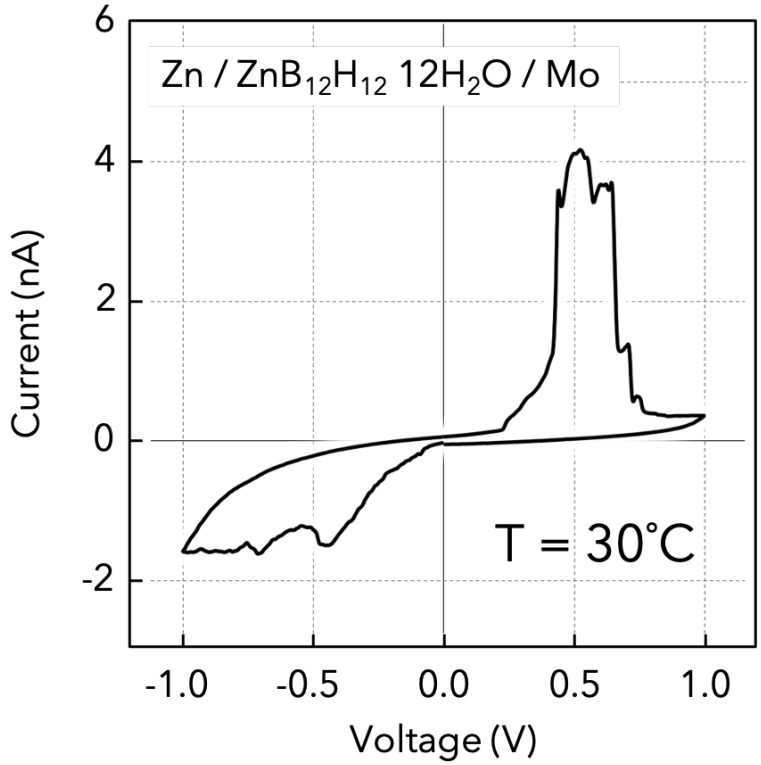

Figure S7. Cyclic voltammograms of Zn | $ZnB_{12}H_{12}$-$12H_2O$ | Mo at 25 °C, scan rate of 20 mV s^{-1}, and voltage range of −1.0 to 1.0 V (vs. Zn^{2+}/Zn) via a microdroplet created with the probe of scanning electrochemical cell microscopy.

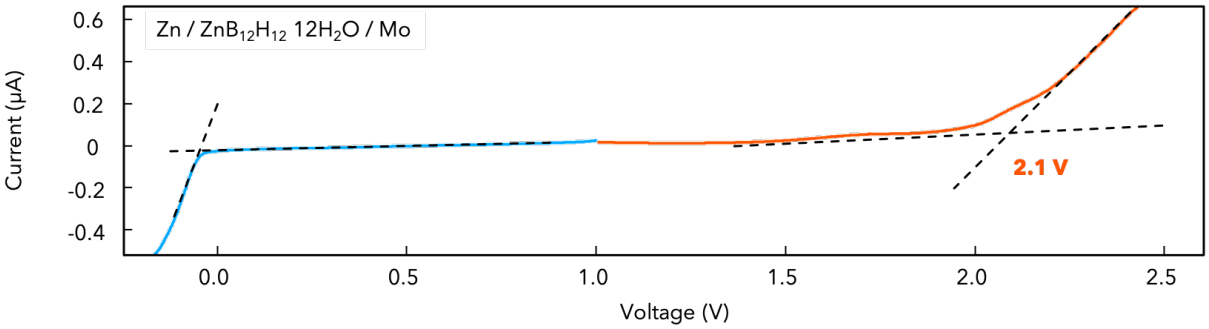

Figure S8. Linear sweep voltammograms of $Zn/ZnB_{12}H_{12}–12H_2O/Mo$ at 50 °C at a scan rate of 1 mV s^{-1} and at a scan range of −0.5 to 2.5 V (vs. Zn^{2+}/Zn).

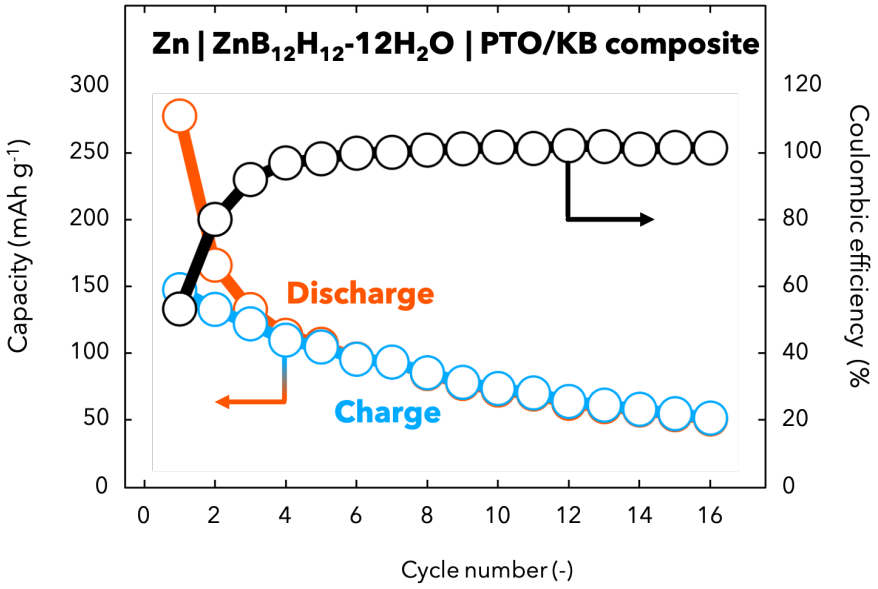

Figure S9. Effects of cycling on the discharge/charge capacities and coulombic efficiency of the Zn-PTO/KB battery.

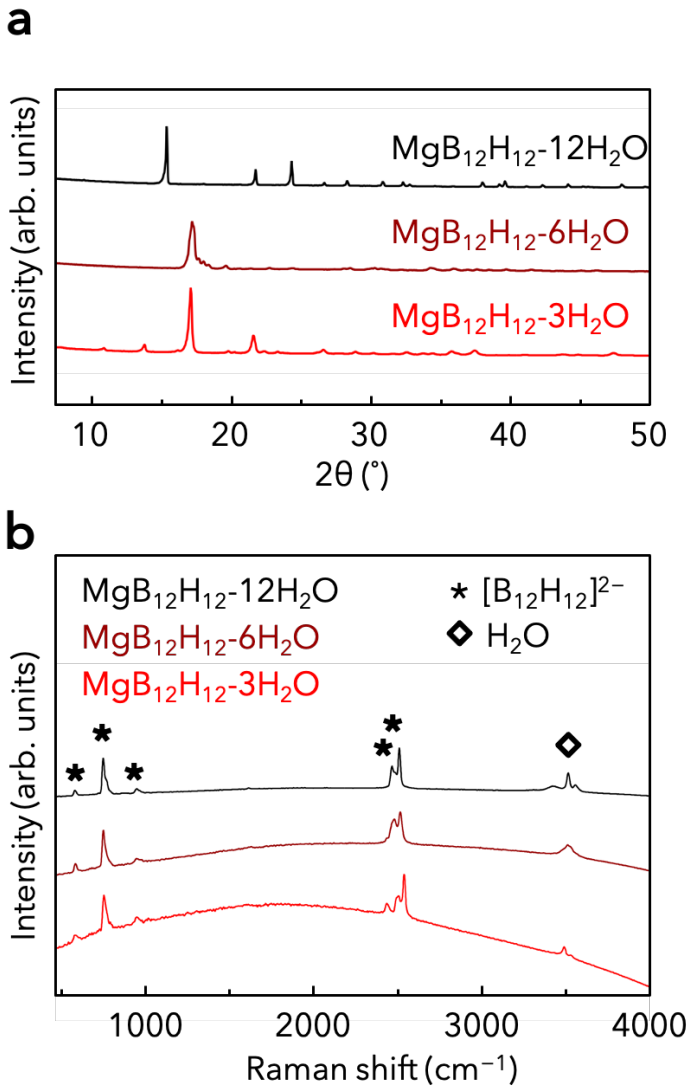

Figure S10. (a) XRD patterns for $MgB_{12}H_{12}$ nH_2O (n = 12, 6, 3). (b) Raman spectra for $MgB_{12}H_{12}$ nH_2O (n = 12, 6, 3).

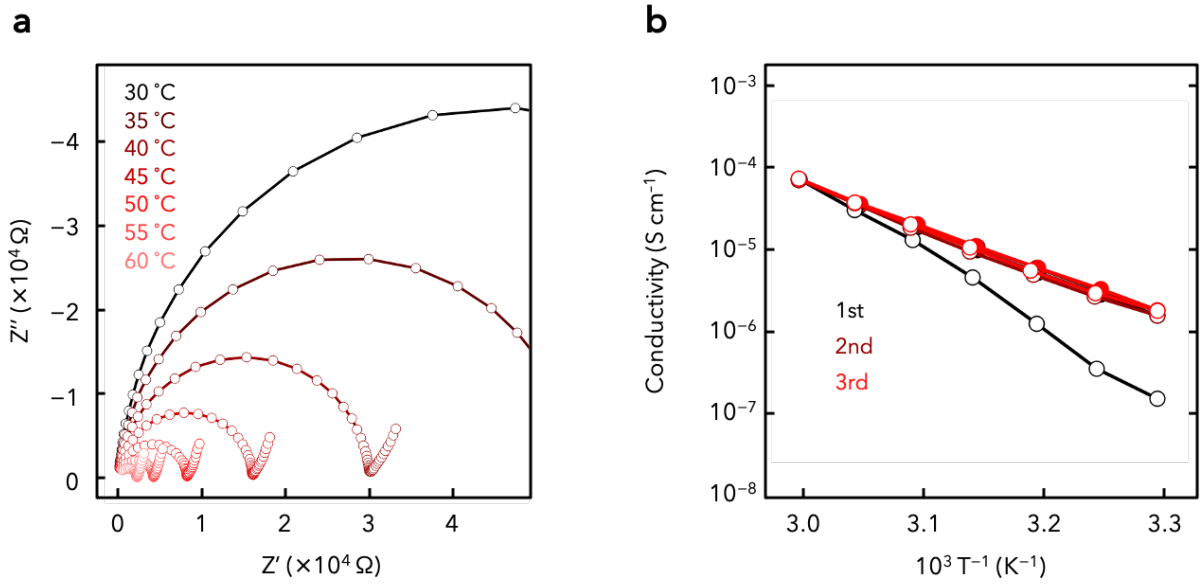

Fig. S11. (a) Nyquist plots for $MgB_{12}H_{12}$–$12H_2O$ measured between 30 and 60 °C with applied frequencies of 4 Hz to 1 MHz. (b) Ionic conductivity of $MgB_{12}H_{12}$–$12H_2O$ obtained by impedance spectroscopy. Black, orange, and blue circles represent the results of the first, second, and third runs, respectively.